Article:
Qin, X, Kräft, T and Goycoolea, FM orcid.org/0000-0001-7949-5429 (2018) Chitosan encapsulation modulates the effect of trans-cinnamaldehyde on AHL-regulated quorum sensing activity. Colloids and Surfaces B: Biointerfaces, 169. pp. 453-461. ISSN 0927-7765

https://doi.org/10.1016/j.colsurfb.2018.05.054

Chitosan encapsulation modulates the effect of trans-cinnamaldehyde on AHL-regulated quorum sensing activity

Xiaofei Qin, [a] Tabea Kräft, [a] Francisco M. Goycoolea, [a]#*

Institute of Plant Biology and Biotechnology, University of Münster, Schlossgarten 3, D-48149 Münster, Germany [a]

#Corresponding author, fm.goycoolea@gmail.com, F.M.Goycoolea@leeds.ac.uk, (F.M. Goycoolea),

*Present address: School of Food Science and Nutrition, Faculty of Mathematics and Physical Sciences, University of Leeds, Leeds, UK

Words: 5864

Abstracts

Quorum sensing (QS) is a chemical communication process involved in the regulation of cooperative and communal activities in bacteria such as virulence production, bioluminescence and biofilm formation. Hence, the inhibition of QS processes has been examined as a promising alternative to deal with bacterial pathogens using antibiotic-free-based therapies. Trans-cinnamaldehyde (CA) is an intensively studied compound that proved to inhibit QS activity by decreasing the DNA-binding ability of LuxR while inhibiting acylhomoserine lactone production. In this work, chitosan based nanocapsules laden with a high concentration of CA were applied to a transformed E. coli Top 10 strain fluorescence-based reporter. Colloidal stability was assessed in M9 medium. The encapsulation efficiency of hydrophobic compound CA (20 mM; >37%)

was greaterer than hydrophilic compounds vanillin (20 mM; ~20%) and caffeine (20 mM; ~10%). Biosensor assay shows us that CA-laden nanocapsules exhibit higher QS inhibition activity than free CA and CA-laden nanoemulsions. This result indicated that nanocapsules can interact with E. coli via electrostatic interaction, while thus effectively deliver CA to the bacteria. We reasoned that electrostatic adsorption of the chitosan-coated noncapsules to the bacterial cell envelope, is the mechanism that underpins the observed enhancement of the QS inhibition activity.

Keywords: quorum sensing; chitosan-based nanocapsules; trans-cinnamaldehyde; electrostatic interaction; quorum sensing inhibition

Introduction

The indiscriminate use of antibiotics to deal with human and animal infections world-wide has resulted in multiple drug resistant (MDR) by many pathogenic bacterial strains. For example, Mycobacterium tuberculosis resistant to therapeutic concentrations of the streptomycin were found to arise during patient treatment [1,2]. The World Health Organization (WHO) has urged the world to implement consolidated efforts to avoid regressing to the pre-antibiotic era by the spreading of antimicrobials resistance, and researchers world-wide are encouraged to discover novel approaches to deal with this global challenge [3].

Bacteria evolved mechanisms of communication that are mediated by the synthesis and exquisite detection of chemical signals termed autoinducers (AIs). Synchronous phenotypic responses take place at the population level [4,5]. These responses include biofilm formation, toxins production, bioluminescence, swarming motility, among other [6,7]. Altogether, the phenomena whereby bacteria synthesize and detect AIs, as a function of cell density, and activate gene expression in a

concerted manner are known as quorum sensing (QS) [8]. QS can be regarded as a cell-to-cell communication process, comprised by a "speaking" module (the synthesis of AIs) and a "listening" module (the detection of AIs). Almost since its discovery, it was also recognized that to interfere with bacterial QS, would be an alternative strategy to the use of antibiotics that may circumvent the development of drug resistance [9]. At least four approaches to disrupt QS have been pursued since, namely: 1) inhibition of the AIs synthesis [10]; 2) enzymatic degradation of the AIs [11,12]; 3) use of materials (e.g., films, hydrogels or nanoparticles) that selectively adsorb or "quench" AIs [13,14]; or 4) use of compounds that mimic AIs with affinity for the proteins (e.g., LuxR) involved in their detection [15]; and. In this study, we have addressed a combination of approaches 3) and 4).

Chitosan describes a family of aminosaccharides that has gained traction over the past decade or so in drug and gene delivery due to its biodegradability, biocompatibility, and nontoxic properties [16]. Chitosans are well studied for their antimicrobial activity since the polycationic amines of chitosans interact with negatively charged residues of macromolecules at the cell surface of bacteria, subsequently inhibiting bacterial growth [17-20]. In recent study, chitosan shows potential anti-QS activity by disturbing biofilm formation and inhibiting C. violaceum violacein production [21]. Chitosan-based nanomaterials have also shown biological activities against microorganisms, including bacteria and fungi activity [22,23]. Recent studies have shown that the enhanced antimicrobial activity of chitosan-based NPs is related to the increase of surface area to volume ratio as the particle size decreases [63,64]. In a series of accompanying studies carried out in our laboratories, we have addressed the antibacterial activity of a purified chitosans of varying degree of N-acetylation (DA) and degree of polymerization. We have found that only the chitosans with low DA (~ 12%) reduced the bacterial growth of an E. coli AHL-

reporter strain [24]. Also, we have evidenced that either chitosan in solution [24], ionotropic gelled nanoparticles (NP) [25], or chitosan-coated nanocapsules (NC) [26], depending on the dosed concentration, inhibit QS in the same biosensor strain.

Cinnamaldehyde (CA) is an aromatic aldehyde and the major component of cinnamon oil derived from natural sources such as cinnamon, cinnamon, and cassia leaf [27-29]. It has been known that low concentrations of CA were effective at inhibiting AHL- mediated QS [30]. Moreover, CA and CA derivatives have been shown to inhibit QS activity in various Vibrio spp. by decreasing the DNA-binding ability of LuxR or inhibit AHL production in P. aeruginosa QS system [31-33]. In our related study, we have shown that CA not only inhibits the expression of green fluorescence protein (GFP), but it also retards its kinetics [34]. By contrast with the previous anti-QS studies in P. aeruginosa, we have shown that CA disrupts the QS in the absence of the "QS-speaking" module (i.e., synthesis of AHL) [34]. Indeed, we were able to establish a direct linear relationship between the concentration of CA and the critical onset time of the synchronous "QS-listening" response in the same E. coli AHL-reporter strain used in the present study. For comparison purposes, in the present study, we have also included vanillin and caffeine, as two additional compounds were encapsulated in chitosan-based NC and characterized their physico-chemical properties that including size, zeta potential, polymer dispersion index (PDI) and encapsulation efficiency (EE). In the previous studies, vanillin and caffeine were identified as quorum sensing inhibitors [35,36]. In our laboratory, we demonstrated that those two compounds could inhibit the GFP production of E. coli AHL-reporter strain but had no effect with bacterial growth. Many NP-based antibiotics delivery systems have been extensively explored in various areas that enhance therapeutic effectiveness [37]. However, only few studies have used nanomaterials to enhance or modulate the QS

inhibition activity. To the best of our present knowledge, there have not been studies documenting the development of CA-loaded nanomaterials to test their effectiveness to inhibit the QS activity. In this study, we examined colloidal NC and chitosan-coated nanoemulsion (NE) with an oily core loaded with lipophilic CA. We addressed the effectiveness of these systems as potential carriers of CA able to target E. coli AHL-bioreporter strain and modulate the QS response. We found that chitosan-based NC has high loading efficiency of CA, prolonging the CA release time and enhancing the anti-QS activity.

Result

The physicochemical properties of nanocapsules and nanoemulsions

Figure 1 shows the size and zeta potential of nanoformulations (NM), namely NE and NC. The Z-average diameter of unloaded NC is ~ 149 nm, slightly greater than unloaded NE (Ø ~ 125 nm). Very similar dimensions were also determined in CA-loaded NC (Ø ~ 165 nm), also greater than that of CA-loaded NE (Ø ~ 120 nm). The PDI of all systems was very low ranging from ~ 0.1 to ~ 0.2. Both unloaded and CA-loaded NC had strong positive zeta potential (ζ) that are ~ +50 and ~ +42 mV, respectively. By contrast, the unloaded NE and CA-loaded NE, lacking the chitosan coat, had strongly negative ζ, ~ -40 and ~ -52 mV, respectively.

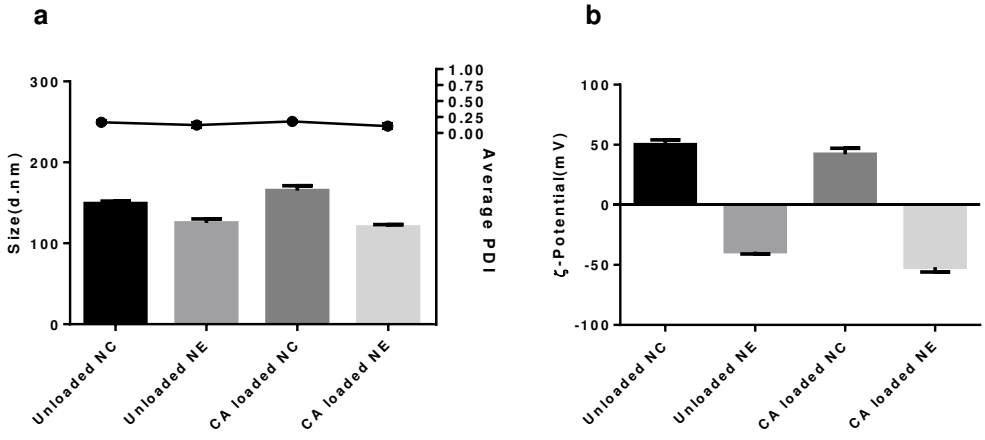

Figure 1. Physicochemical properties of chitosan-coated NC and NE, unloaded or loaded with CA (10 mM). (a) The Z-average diameter and PDI of NC and NE. (b) The zeta-potential of NC and NE (1 mM Potassium chloride, 25ºC).

Physical characterization and encapsulation efficiency of trans-cinnamaldehyde, vanillin and caffeine

The physical properties, encapsulation and loading efficiency of CA-, vanillin- and caffeine-loaded NC and NE are summarized in Table 1. Notice that loading neither CA (~ 6%) nor the more hydrophilic compounds caffeine (~ 2%) nor vanillin (~ 3%) did influence the Z-average size, PDI and ζ values of NC or NE. The Z-average diameter of each formulation ranged from ~ 120 to ~ 160 nm, representing PDI of ~ 0.1 to ~ 0.2. All ζ values of NC are strongly positive (~ +35 to ~ +42 mV), while those of NE are strongly negative (~ -44 to ~ -52 mV). However, the EE values of CA, when loaded 20 mM, in NC (~ 37%) and NE (~ 50%) were notably greater than those of vanillin (EE ~ 19 and 18% in NC and NE, respectively). The lowest EE was registered for caffeine-loaded at the same concentration (20 mM) on both systems, (EE ~ 9% in

both). The EE is significantly increased when encapsulated 10 mM CA in the NM, which are ~ 78% in NC and ~ 82% in NE.

Table 1. Physicochemical characteristics, encapsulation efficiency and loading efficiency of trans-cinnamaldehyde-, vanillin-, or caffeine-loaded nanocapsules and nanoemulsions.

Nanoformulations[1]	Concentration [2] (mM)	Z-average size (d., nm)	PDI	ζ (mV)	EE[3] (%)	LE[4] (%)
CA loaded NC	10	165±6	0.18	+42±5	78±3	5.8±0.23
CA loaded NE	10	120±3	0.11	-52±4	82±2	6.4±0.17
CA loaded NC	20	150±6	0.12	+42±3	37±16	5.5±2.41
CA loaded NE	20	132±3	0.17	-50±6	50±15	7.7±2.32
Vanillin loaded NC	20	146±5	0.12	+39±5	19±10	3.3±1.74
Vanillin loaded NE	20	129±4	0.13	-52±5	18±6	3.3±1.13
Caffeine loaded NC	20	145±6	0.11	+34±2	9±3	2.0±0.68
Caffeine loaded NE	20	125±2	0.10	-44±3	9±4	2.2±0.96

[1] CA= trans-Cinnamaldehyde; NC = nanocapsules; NE = nanoemulsions

[2] Concentration of active molecule

[3] Encapsulation efficiency

[4] Loading efficiency

The stability of nanoformulations in M9 medium

Figure 2 shows the time-evolution average size and PDI measurements of unloaded NC and NE incubated in bacterial culture medium (M9 medium) at 37ºC. Notice that the size and PDI of NC

remained fairly constant during the incubation of both type of systems for 12 h. However, NE grew nearly by two fold during the time course of the assay, namely from ~ 150 nm (PDI ~ 0.2) to ~ 500 nm (PDI ~ 0.4) after 12 h incubation.

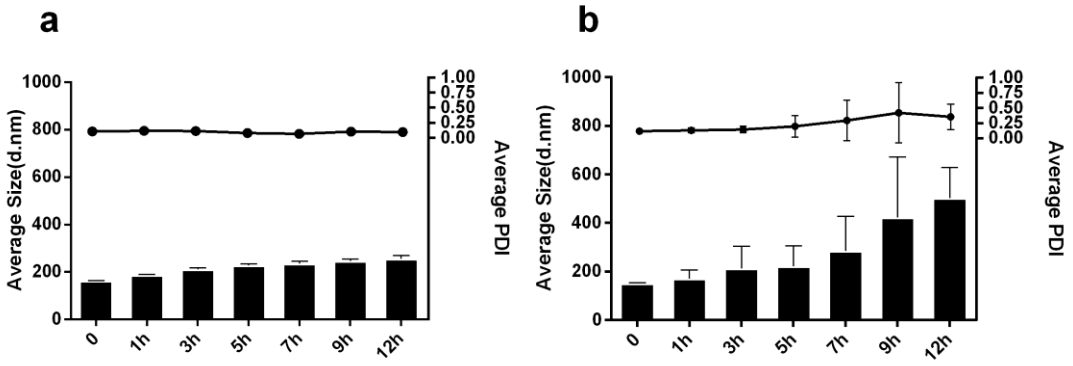

Figure 2. Evolution of diameter (bars) and average polydispersity index (PDI, circles and line) of (a) unloaded nanocapsules, and (b) unloaded nanoemulsions during incubation in M9 medium (at 37ºC) for 12 hours (values are average of three replicates ± s.d.)

Trans-cinnamaldehyde in vitro release assay in M9 medium

The results of the in vitro assay of CA release in M9 bacterial culture medium are shown in Figure 3. Notice that both of the nanosystems released a great amount of CA into the medium (Figure 3a). After 6 h, both the NC and NE released similar amounts of CA (~ 2.46 mM, ~ 24.6%). The data of CA release profiles were further fitted to Korsmeyer-Peppas equation (Eq. 3) [38]. It can be observed that both the NC (R^2 = 0.9680) and NE (R^2 = 0.9555) both afforded high correlation, with slope exponent n values for NC and NE of 0.33 and 0.23, respectively (Figure 3b)

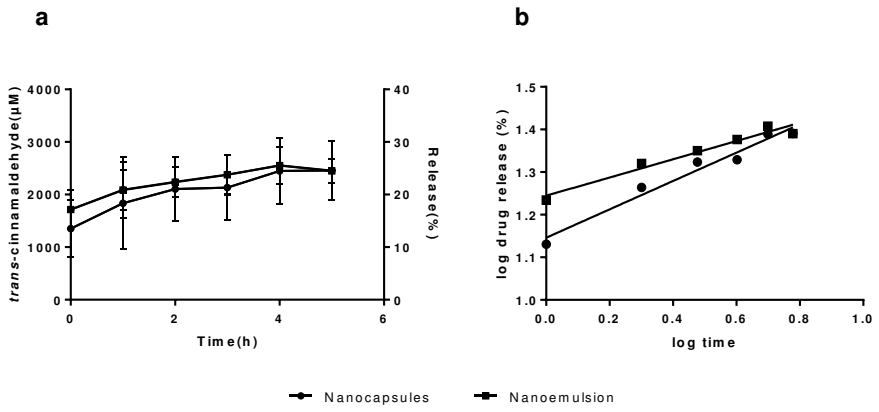

Figure 3. (a) In vitro CA release in M9 bacterial culture medium (37ºC) with a concentration of 10 mM CA in the NC and NE. (b) The double logarithmic representation of the data. Data are mean values ± SD (n = 3).

E. coli Top10 biosensor assay

We examined the influence of CA, chitosan at different concentration, blank and CA-loaded NC and NE (CA ~ 0.5 mM) on the response of the AHL E. coli biosensor assay. This response included the evolution of the fluorescence intensity, the OD_{600} (proportional to bacterial growth). The influence of adding increasing concentrations of CA were evaluated in the E. coli biosensor assay for 4.5 h (Fig. 4a). Notice in Figure 4a that there was no inhibition of bacterial growth at different concentrations of CA. Also, at 0.05 mM, there was no effect on the intensity of fluorescence associated to GFP production. However, a significant decrease in the normalized fluorescence intensity/OD_{600} response was observed in a dose-dependent manner in the range of CA concentration from 0.25 to 1 mM respectively. The anti-QS activity of the blank and CA-loaded NE and NC is shown in Figure 4b and 4c, respectively. In these experiments, the same concentrations of NE and NC were applied. Also, chitosan in solution at concentration of 0.05 (i.e., the same concentration applied in the NC) and at 0.1 mg/mL were evaluated, and the results

are shown in Figure 4d. Neither the reduction in the fluorescence intensity nor in the bacterial growth (OD_{600}) was observed upon treatment with blank NE and NC, nor with chitosan when applied at the same concentration as that in the NC (Figure 4b and 4d, respectively). Both CA-loaded NC and NE did not exert toxicity as evidenced by the bacterial growth profiles, though both retarded the abrupt rise in the normalized fluorescence intensity/OD_{600} response after the first hour in the biosensor assay. However, the CA-loaded NC could decrease the normalized fluorescence intensity/OD_{600} response after ~ 4.5 h, while CA-loaded NE had no discernible effect at this stage of growth.

In order to establish quantitative comparisons, we selected the average of the last ten fluorescence intenisty/OD_{600} and OD_{600} measurements (i.e., the data corresponding to the last hour of the experiment, when the growth rate is assumed to have entered in the stationary phase). The relative QS activity is thus defined as the ratio of the fluorescence intensity/OD_{600} of a given treatment with respect to that of the control (i.e., only AHL). Therefore, theoretically a relative QS value equals to one means that the evaluated compound has no QS inhibition activity, as it neither an effect on GFP expression nor on bacterial growth. In turn, relative QS values lower than one is diagnostic of QS inhibition so long as the OD_{600} does not decrease. To establish statistical comparisons, we referred to CA at 0.05 mM, because it had neither effect on QS activity nor on bacterial growth. Figure 5a shows that none of samples exhibited a significant effect ($p < 0.05$) on bacterial growth. In turn, Figure 5b shows that when CA was applied at a concentration of 0.25 mM it inhibited the relative QS response by ~ 22.0% ($p < 0.05$). Also in this case, a pronounced dose-response effect was clearly observed on the values corresponding to CA concentrations of 0.5 or 1.0 mM, that reduced significantly the QS activity by 43.4% ($p < 0.0001$) or 79.8% ($p < 0.0001$), respectively.

CA-loaded NC, when applied at a CA concentration of 0.5 mM, also inhibited significantly the QS activity by 25.5% ($p < 0.01$), though with lower magnitude than when CA was applied at the same dose in the free form. In contrast, the E. coli biosensor assay did not detect QS inhibition activity neither on blank NC nor NE systems, CA-loaded NE nor for two different doses of chitosan (Figure 5b).

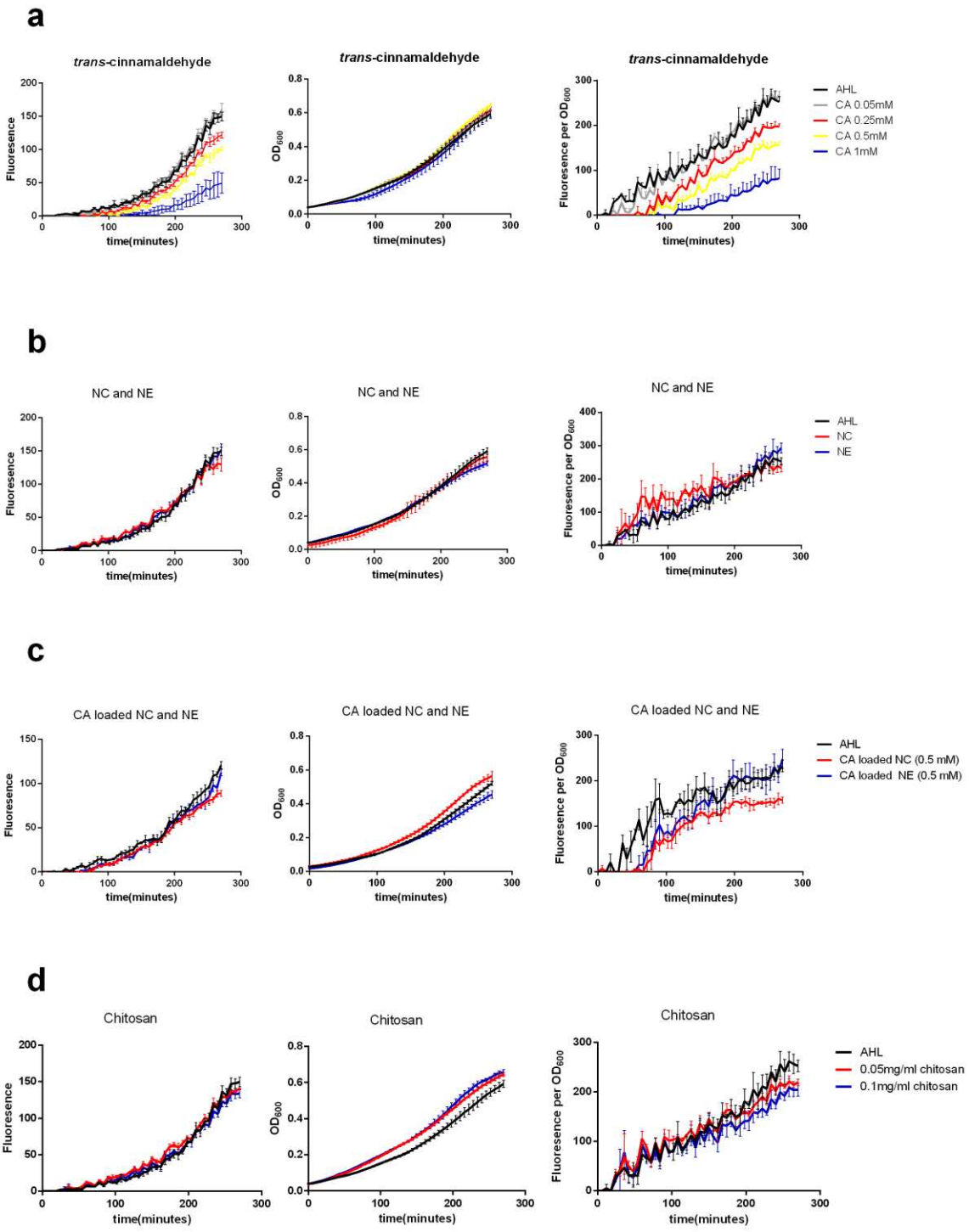

Figure 4. Dependence of the fluorescence intensity, growth (OD_{600}) and normalized fluorescence intensity/OD_{600} responses during the growth of the E. coli biosensor upon treatment

with varying samples of: a) trans-Cinnamaldehyde (CA) at 0.05, 0.25, 0.5 and 1 mM; b) Blank (unloaded) nanocapsules (NC) and nanoemulsions (NE); and c) trans-Cinnamaldehyde-loaded nanocapsules (NC) and nanoemulsions (NE); and d) Chitosan in solution at 0.05 and 0.1 mg/mL. The individual traces represent the average of three independent biological experiments with at least three technical replicates.

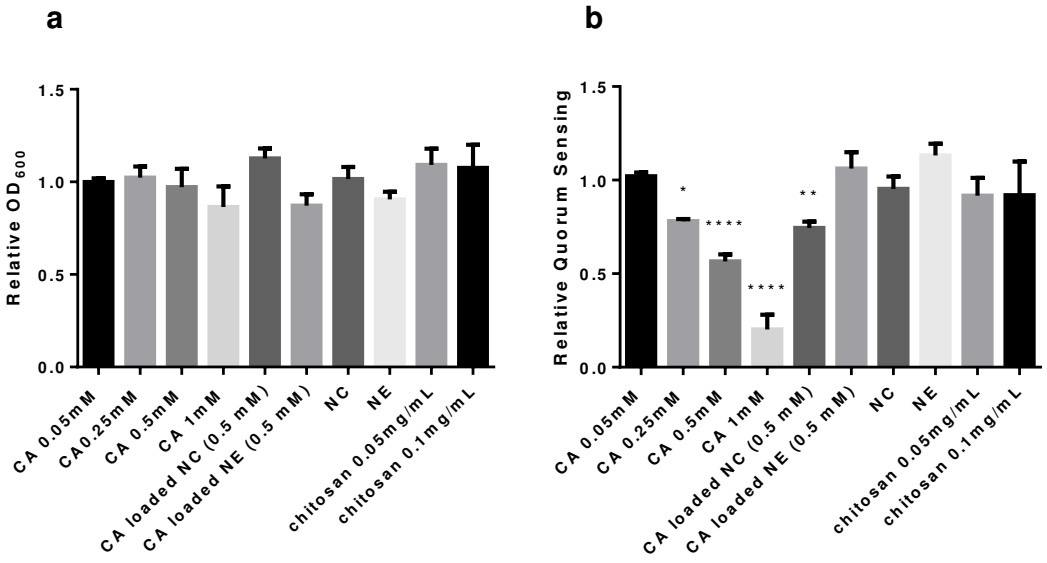

Figure 5. Effect of different treatments on a) Relative bacterial growth (OD_{600}); and b) Relative quorum sensing (fluorescence intensity/OD_{600} ratio) as assessed on a E. coli Top 10 (psb1a3:BBa_T9002) AHL-reporter biosensor strain. Key: CA = trans-Cinamaldehyde, NC = Nanocapsules, NE = Nanoemulsions. t-Test statistical comparisons with respect to 0.05 mM CA (values represent averages ± SD of three independent biological experiments with at least three technical replicates; *$p < 0.05$, **$p < 0.01$, ***$p < 0.001$ and ****$p < 0.0001$).

Discussion

Drug-loaded nanoparticles based on polymers or other materials are a useful platform that prolong the release time, thereby reducing side effects and systemic toxicity, associated with many drugs. Besides, when nanoparticles are functionalized at their surface with recognizing (biotargeting) motifs, this can enhance the homing and drug release efficiency at the site of interest [39,40].

In the preset study, we have investigated the physical properties, colloidal stability and biological activity on an E. coli AHL-reporter strain of NC and NE, either blank or loaded with CA. Firstly, we determined the physical characteristics of the blank NE and NC in terms of size, zeta potential and stability in M9 bacterial culture medium. Previous studies showed us that the size of chitosan-based NC was admittedly affected by the degree of polymerization and DA. NC coated with chitosan of low degree of polymerization (LDP) exhibited slightly lower Z-average sizes than the high degree of polymerization (HDP) chitosan-coated NC, our results agree with such previous reports [41]. The size of NE (~ 125 nm) was somewhat smaller than that of NC, also in line with previous reports. This is the expected consequence of the lack of the chitosan shell in NE.

The stability of NC and NE during their incubation in M9 medium was assessed by measuring the particle size using dynamic light scattering at varying time intervals up to 12 h at 37ºC. M9 medium is commonly used to grow E. coli in the presence of glucose or other carbon sources. This medium also contains different ions such as divalent cations (e.g., calcium and magnesium) and other components (e.g., casamino acids and thiamine). Figure 2b shows that NE is unstable in the M9 medium at 37ºC for 12 h incubation. In our NE system, lecithin is the emulsifier that

plays a role in making NE stable in the water through repulsive electrostatic interactions and steric hindrance [42]. However, there are various factors that affect the stability of NE. These factors like the temperature, ionic strength, volume fraction, solubility, components chemistry, emulsifier concentration can make the destabilization of NE, such as Ostwald ripening, coalescence, and flocculation [42]. Furthermore, it is well known that divalent cations (such as calcium and magnesium) specifically interacts with lecithin polar groups [43,44]. Our results suggest that the divalent cations in the M9 medium interact with lecithin and interfere with the zeta potential of the NE to induce the destabilization of NE. In contrast, colloidal stability study of NC revealed that NC is stable in the M9 medium (Fig. 2a). Previous studies showed that chitosan-based NC is anomalous stable when immersed in saline media because of the hydration forces, a short-range repulsive interaction [41,44]. Thus, in our NC system, chitosan located in the shell of NC avoids the direct interaction between divalent cations with the lecithin layer, and the hydration forces played a crucial role in keeping NC stable in M9 medium [44].

Furthermore, three different drugs were loaded into the NC and NE (20 mM), namely caffeine, vanillin and CA. On each of these drugs, with different log $P_{octanol/water}$ parameters. The log $P_{octanol/water}$ of caffeine (- 0.25), vanillin (1.21) and CA (1.9) were cited from the literature [45-47]. It was reported that the encapsulation efficiency of drugs correlated to the partition coefficient between 1-octanol and water [48]. In our NM systems, the NE with an oily core and NC with an oily core and chitosan shell assembly by spontaneous emulsification can carry hydrophobic and hydrophilic molecules. Our study shows that the higher value of log $P_{octanol/water}$, the higher encapsulation efficiency for both NC and NE systems (R^2 = 0.87 of NC, R^2 = 0.75 of NE). There are several ways to make the drug loaded on the nanoparticles, such as encapsulation and dispersion of the drug in the polymer, adsorption of the drug onto the surface of the nanoparticles

and chemical binding of the drug to the polymer [49]. As in our NM systems, the core is Miglyol oil which main composition is caprylic/capric triglyceride, forming the hydrophobic core. Thus it is not surprising that the hydrophobic compound CA can be most encapsulated in the systems and the systems contains least hydrophilic compound caffeine. Given that the drug can be encapsulated into the Miglyol oily core, it was reported that amphiphilic drugs could be embedded into the phospholipid bilayer of the lecithin which means that lecithin also an important factor to load drugs [48]. Previous studies have suggested that hydrogen bonding between the two β-(1→4)-2-amino-D-glucose units of chitosan and vanillin leads to the formation of stable complexes [50]. By use FTIR spectroscopy analysis, other reports have suggested that the aldehyde group of vanillin cross-links with chitosan amino functions. As an result of such cross-linking reaction, the formation of nanoparticles has been reported [51] [52]. Regarding caffeine, FTIR analysis has revealed that the interaction with chitosan can take place by trapping and coating chitosan-based NPs [53]. These studies have indicated that chitosan-based systems are amenable for loading different types of drugs. However, our own experiments show that the NC comprising chitosan, do not increase the encapsulation efficiency of neither caffeine, vanillin nor CA, when compared with that observed for NE, devoid of chitosan. This suggests that in NC and NE, the nature of the coating shell is not the main factor that influences the encapsulation efficiency, but rather the Miglyol oily core, is the most important factor. Previous reports have shown that the encapsulation efficiency depends on the character of the drugs, the physical and chemical properties of encapsulating polymers, solvent systems, polymer–drug interactions, medium pH, preparation methods, and electrolyte addition [48,54-56]. Also, processing parameters including stirring, homogenization, sonication, and equilibration times are of important factors [57-60]. We attribute the low encapsulation efficiency of caffeine

in our NC and NE systems to its hydrophilic character that has a very low affinity to Miglyol oil. Several ways can be used to increase the encapsulation efficiency of the hydrophilic drug. By lowering the pH of the outer media, the drug entrapment efficiency of water-soluble sodium cromoglycate was dramatically increased from 15% to 70% [55]. Gregor Dördelmann et al showed that calcium phosphate increases the encapsulation efficiency of hydrophilic drugs [59]. All those studies give us the hint to increase the encapsulation efficiency of the hydrophilic compound in our systems. In our experiment, the concentration of CA also affected the encapsulation efficiency, as 20 mM CA loaded into the NM, only ~ 37% CA in the NC and 50% CA in the NE. Thus, in an attempt to increase the encapsulation efficiency of CA, we decreased the loaded concentration to 10 mM. This measure enabled to increase the encapsulation efficiency for both of NC (~ 78%) and NE (~ 82%). Even through the encapsulation efficiency is different with different concentrations of loaded CA, the loading efficiency is similar (~ 6%), thus suggesting that this might be the maximal loading capacity for both systems.

A total of ~ 80% of loaded CA (10 mM) is encapsulated in both NC and NE. This means that the remaining amount (~ 2 mM) is in the free form. The results of the QS biosensor assay showed that at a concentration of free CA of ~ 0.1 mM, it had no significant effect on the fluorescence intensity/OD_{600} response (Fig. 4 and Fig. 5). Due to the high loading efficiency and the well-known QS inhibition activity of CA, we opted to address in further detail the effect of encapsulation on this compounds in NC and NE. The anti-QS study based on E. coli biosensor assay revealed that CA could reduce the fluorescence intensity at high concentration but without affecting the bacterial growth (Fig. 4a and Fig. 5). Previous studies have investigated the mechanism of inhibition of the QS activity of CA [31,32]. The E. coli top 10 reporter strain used in our studies constitutively expresses LuxR receptor, but it is active only in the presence of the

exogenous autoinducer signaling molecule $3OC_6HSL$. Our data agree with previous studies that have suggested that in the presence of CA, the binding of transcriptional regulator LuxR to its promoter sequence is affected, thus leading to a reduction on GFP expression [31].

An important caveat of our study was avoiding chitosan-based NC to inhibit the bacterial growth during the QS activity assays. To this end, the specific chitosan was selected from a series of chitosans of varying DA and Mw identified in a parallel study, that revealed that a Chitosan MDP DA30 (DA 42% and M_w 115 kDa) did not affect the bacterial growth, nor the QS activity [24]. In the present study, we confirmed that the chitosan used and the chitosan-based NC had no toxic effect on the E. coli strain used (Figure 4b, 4d and 5). The biosensor assay of CA-loaded NC, and NE (Figure 4c and 5), showed that only CA loaded NC reduced the GFP production but CA loaded NE had no effect with anti-QS activity. In vitro release studies (Figure 3) showed that CA release trend fits a linear regression in a double logarithmic plot, the value n exponent < 0.45 indicates the Fickian diffusion is the mechanism of CA release [61]. The similar values of the n exponent in NC (0.33) and NE (0.23) indicated that chitosan on the surface of NC did not affect the CA release behavior compared to the NE. As CA released out of the NC and NE up to 2.46 mM 6 h later which means the final concentration of CA in biosensor assay is 0.123 mM. The biosensor assay (Figure 5) showed that free CA at a lower concentration of 0.25 mM ($p < 0.05$) inhibits the QS activity by 22.0%, whereas CA-loaded NC ($p < 0.01$) inhibits the QS activity by 25.5%. The stronger inhibition of the QS activity observed for the CA-loaded NC, even though the free CA contents in CA-loaded NC environment after 6 h is 0.123 mM (Figure 5b; notice that this is less than the concentration of free CA, 0.25 mM), is diagnostic that the NC are able to deliver their payload directly to the bacteria. More importantly, the CA-loaded NC that contains a high concentration of CA (i.e., ~ 80% encapsulation efficiency) is bound to prolong the CA

releasing time, thus to achieve a more sustained QS inhibition activity, than when CA is administered in the free form. By contrast, CA-loaded NE that also contain a high concentration of CA, showed no effect on the QS bacterial activity (Fig. 4c and Fig. 5b). We have reasoned this result as the consequence of the surface electrical charge of each of the nanosystems. Figure 1b shows that NC has a highly positive zeta potential, whereas NE has a highly negative zeta potential. We know that bacteria surface is also negatively charged [26]. Hence, the NC are likely to interact with bacteria via electrostatic interactions. Thus, NC can target the bacterial surface and enhance the CA anti-QS efficiency, by the favorable electrostatic interaction between oppositely charged surfaces of NC and bacteria.

Conclusion

Here we show that chitosan-coated NC are more stable than NE in the M9 bacterial culture medium as in the presence of chitosan that forms the hydration forces to make NC stable in saline media. Chitosan-based NC can be used as a vehicle to deliver the hydrophobic drug target on the bacterial surface and enhance their anti-QS activity. High concentration of CA can be encapsulated into the NM systems to prolong the drug release time. Further investigations will increase the encapsulation efficiency of hydrophilic drugs caffeine and vanillin as our previous studies suggested that those two drugs also showed strong anti-QS activity in E. coli top 10 strain. Further studies can also be envisaged to involve the co-loading of NC with CA and vanillin or caffeine to increase their anti-QS activity.

Materials and methods

Materials

The sample of chitosan we used was a gift from Mahtani Chitosan Pvt. Ltd., India. The molecular weight of 115000 Da was determined by HPSEC-MALLS and the degree of acetylation of 42% was determined by ^{1}H-NMR spectroscopy. Miglyol 812N was from Sasol GmbH (Witten, Germany); N-(β-ketocaproyl)-DL-homoserine lactone ($3OC_6HSL$), CA and all other chemicals were of analytical grade and were from Sigma–Aldrich Chemie GmbH (Hamburg, Germany).

Preparation of the nanoformulations

Chitosan-based nanocapsules (NC) were prepared following the spontaneous emulsification technique, according with the original protocol of Calvo et al with slight modifications [62]. The nanoemulsions (NE) were prepared using an identical protocol as for the NC, but the aqueous phase consisted only of milli-Q water. To prepare the CA-loaded NC and NE the protocol were identical as for the blank systems, but, 10 mM ethanolic CA stock was mixed with 10 mL ethanol and added in the organic phase. The CA, caffeine and vanillin-loaded NC and NE (CA, caffeine and vanillin are at 20 mM) were prepared with the same method as above described but with the 10 mL of 20 mM ethanolic compounds.

Size and zeta potential

The intensity size (hydrodynamic diameter) distributions of the NC and NE were determined by dynamic light scattering with non-invasive back scattering (DLS-NIBS) at 25 °C. A Zetasizer NanoZS instrument (Malvern Instruments Ltd., Worcestershire, UK) equipped with a 4 mW

helium/neon laser (λ = 633 nm), and detection was at an angle of 173° was used for these measurements. The zeta potential was measured by phase analysis light scattering and mixed laser Doppler velocimetry (M3-PALS) using the same instrument. The samples were diluted 1:100 with a 1mM KCl solution.

Stability assay

A 10 µL aliquot of NC and NE was transferred to cuvettes containing 990 µL of M9 medium previously equilibrated at 37ºC. At appropriate time intervals of 1 h and the whole testing is 12 hours, mean particles size and PDI of NC and NE are analyzed by dynamic light scattering using the Malvern Zetasizer NanoZS instrument as described above.

High-performance liquid chromatography (HPLC) with UV detection

CA was analysed by HPLC-UV. To this end, we used a Jasco HPLC system (Jasco GmbH, Gross-Umstadt, Germany) equipped with three-line degasser (DG-2080-53), a ternary gradient unit (LG-2080-02S), a semi-micro HPLC pump (PU-2085Plus), an autosampler (X-LC™ 3159AS), and an intelligent column thermostat (CO-2060 Plus). The stationary phase was a Kinetex C-18 reversed phase column (2.6 µm, C18, 50 × 2.1 mm, S/N 539947-37; Phenomenex, Torrance, USA) and a UV/Vis detector (X-L™ 3075UV). A mixture of water (A) and acetonitrile (B) was used in gradient mode as the mobile phase at a flow rate was 0.6 ml/min, gradient elution (0-1.7 min: 70% A and 30% B, 1.7 min-2.5 min: 50% A and 50% B, 2.5 min-3 min: 70% A and 30% B), CA was detected at λ=285nm. Vanillin was also analyzed with same instrument, but in this case the mobile phase was a mixture of water (A) and methanol (B) in gradient mode at a flow rate was 0.4 ml/min, gradient elution (0-3 min: 90% A and 10% B, 3 min-4 min: 10% A and 90% B, 4 min-6 min: 90% A and 10% B), vanillin was detected at λ =

231 nm. As for caffeine analysis, the mobile phase was a mixture of 30% water and 70% methanol in isocratic mode as the mobile phase at a flow rate was 0.3 ml/min and UV detection was at λ = 275 nm.

Encapsulation efficiency

The CA-, vanillin- and caffeine-loaded NC and NE were partitioned by ultracentrifugation (Mikro 220 R, Hettich GmbH & Co. KG, Tuttlingen, Germany) at 16,000 rpm for 1 h at 15ºC, and the CA, vanillin and caffeine content of the subnatant was determined by HPLC-UV as described above. The encapsulation efficiency was calculated as the difference between the total amount of drug incorporated in the formulation and the amount present in the subnatant.

$$\text{Encapsulation efficiency} = \frac{C\text{total} - C\text{subnatant}}{C\text{total}} \times 100\% \quad (1)$$

$$\text{Loading efficiency} = \frac{\text{Entrapped Drug}}{\text{Total drug loaded nanoformulations weight}} \times 100\% \quad (2)$$

In vitro CA release assay

An 800 μL aliquot of each formulation was transferred to a dialysis tube (Pure-a-lyzer Maxi 0.1–3.0 mL, Mw cut-off = 6 kDa, Sigma-Aldrich GmbH, Steinheim, Germany) and placed in a glass beaker containing 79.2 mL M9 medium previously equilibrated at 37ºC in an incubator. Every hour, a 500 μL aliquot of medium was removed and replaced with the same volume of M9 medium. The CA content of the aliquots was determined by HPLC as described above. The transport of CA from the nanoformulations into the medium was analyzed by fitting the data to the empirical equation

$$M_t/M_\infty = kt^n \quad (3)$$

where M_t is the mass of CA released at time t. The parameter M_∞ represents the total mass of CA to be released and k is a constant that depends on the structural characteristics of the NM and the solvent/material interactions. The exponent n is used to indicate the type of diffusion.

Bacterial strains

E. coli Top10 was transformed with the plasmid pSB1A3-BBa_T9002, carrying the BBa_T9002 genetic device (Registry of Standard Biological Parts: http://parts.igem.org/Part:BBa_T9002), kindly donated by Prof. Anderson Lab (UC Berkeley, USA). The sequence BBa_T9002 was introduced by chemical transformation (Invitrogen, Life Technologies Co., UK) and stored as a 30% glycerol stock at –80ºC. The transformed strain is a biosensor that can respond to the N-(3-oxohexanoyl)-L-homoserine lactone ($3OC_6HSL$) and is the same strain used in accompanying studies [25, 34]. The sequence BBa_T9002, comprised the transcription factor (LuxR), under the control of the lux pR promoter from Vibrio fischeri, which is constitutively expressed but it is active only in the presence of the exogenous cell-cell signaling molecule $3OC_6HSL$. The fluorescence biosensor was calibrated for different $3OC_6HSL$ concentrations as previously described [34].

Growth media and conditions

Bacterial strains were cultivated using on Luria-Bertani (LB) and M9 minimal medium purchased from Becton, Dickinson and company, Germany. We inoculated 10 mL of LB broth supplemented with 200 µg/mL ampicillin with a single colony from a freshly streaked plate of Top10 containing BBa_T9002 and incubated the culture for 18 h at 37ºC, shaking at 100 rpm. Each culture was then diluted 1:1000 into 20 mL M9 minimal medium supplemented with 0.2% casamino acids and 1 mM thiamine hydrochloride plus 200 µg/mL ampicillin (AppliChem

GmbH, Germany). The culture was maintained under the same conditions until the OD_{600} reached 0.15 (~ 5 h). Then we mixed 500 µL overnight culture and 500µl 30% sterile glycerol together in the white plastic vials and store them in the -80 degree freeze. Before the biosensor assay, we prepared the bacteria cultivation that we took the 40µL bacterial from the white plastic vials and cultivated it with 20 mL M9 medium plus 200 µg/mL ampicillin, the culture will be used for biosensor assay until the OD_{600} reached 0.04 ~ 0.07 (~ 4 h).

E. coli Top10 biosensor assay

The $3OC_6HSL$ was dissolved in acetonitrile to a stock concentration of 100 mM and stored at –20ºC. Prior to each experiment, serial dilutions from the stock solution were prepared in water to produce solutions with a concentration ranging from 100 mM to 10 nM. For the biosensor assay, a 5 µL aliquot of the 100 mM $3OC_6HSL$ stock solution was diluted with milli-Q water to a final concentration of 10 nM. We then mixed 10 µL $3OC_6HSL$ aqueous solution with 10 µL of the samples in the wells of a flat-bottomed 96-well plate (Greiner Bio-One, cat. # M3061) and each well was then filled with 180 µL aliquots of the bacterial culture to test for QS inhibition activity. Several controls were also set up. Blank 1 contained 180 µL of M9 medium and 20 µL of miliQ water to measure the absorbance background. Blank 2 wells contained 180 µL of bacterial culture and 20 µL of miliQ water to measure the absorbance background corrected for the cells. Finally, positive control wells contained 10 µL of water plus 10 µL $3OC_6HSL$ solution and 180 µL of the bacterial culture to measure the fluorescence background. In order to remove the effect of samples themselves with OD_{600} and fluorescence, we added 10 µL $3OC_6HSL$ solution with 10 µL of the samples in the wells and each well was then filled with 180 µL M9 medium to test the samples control in biosensor assay.

The plates were incubated in a Safire Tecan-F129013 Microplate Reader (Tecan, Crailsheim, Germany) at 37ºC and fluorescence measurements were taken automatically using a repeating procedure (λ_{ex} = 480 nm and λ_{em} = 510 nm, 40 µs, 10 flashes, gain 100, top fluorescence), absorbance measurements (OD_{600}) (λ = 600 nm absorbance filter, 10 flashes) and shaking (5 s, orbital shaking, high speed). The interval between measurements was 6 min. For each experiment, the fluorescence intensity (FI) and OD_{600} data were corrected by subtracting the values of absorbance and fluorescence backgrounds and expressed as the average for each treatment. All measurements were taken in triplicate.

Statistical analysis

Statistical analysis was carried out using Prism v6.0c (GraphPad Software Inc., La Jolla, USA). All the experiments were performed in triplicates to validate reproducibility and the p values were calculated statistically by Student's t test. Values were expressed as mean ± SD. Comparison analysis was performed between tests and control.

Acknowledgements

XQ was recipient of a fellowship from China Scholarship Council (CSC). We are indebted to Celina Vila for the E. coli E. coli Top 10 QS strain, and to Antje von Schaewen for the generous access to the Safire Tecan-F129013 Microplate Reader.

References

1. J. Davies, D. Davies, Origins and evolution of antibiotic resistance. Microbiol Mol Rev. 74 (2010) 417-433.
2. J.M.A. Blair, M.A. Webber, A.J. Baylay, D.O. Ogbolu, L.J.V. Piddock, Molecular mechanisms of antibiotic resistance. Nat Rev Microbiol. 13 (2015) 42-51.
3. http://www.who.int/would-health-day/2011/en/.
4. C.M. Waters, B.L. Bassler, Quorum sensing: Cell-to-cell communication in bacteria. Annu Rev Cell Dev Biol. 21 (2005) 319-346.
5. W. Ng, B.L. Bassler, Bacterial Quorum-Sensing Network Architectures. Annu Rev Genet. 43 (2009) 197-222.
6. C.D. Sifri, Quorum Sensing : Bacteria Talk Sense. Clin Infect Dis. 47 (2008) 1070-1076.
7. L.C.M. Antunes, R.B.R. Ferreira, M.M.C. Buckner, B.B. Finlay, Quorum sensing in bacterial virulence. Microbiology. 156 (2010) 2271-2282.
8. W.C. Fuqua, S.C. Winans, E.P. Greenberg, Quorum sensing in bacteria: The LuxR-LuxI family of cell density- responsive transcriptional regulators. J Bacteriol. 176 (1994) 2269-275.
9. B. LaSarre, M.J. Federle, Exploiting Quorum Sensing To Confuse Bacterial Pathogens. Microbiol Mol Biol Rev. 77 (2013) 73-111.
10. T.T. Hoang, H.P. Schweizer, Characterization of Pseudomonas aeruginosa enoyl-acyl carrier protein reductase (FabI): A target for the antimicrobial triclosan and its role in acylated homoserine lactone synthesis. J Bacteriol. 181 (1999) 5489-5497.

11. Y. Dong, J. Xu, X. Li, L. Zhang, AiiA , an enzyme that inactivates the acylhomoserine lactone quorum-sensing signal and attenuates the virulence of Erwinia carotovora. PNAS. 97 (2000) 3526-3531.
12. S.J. Lee, S. Park, J. Lee, D. Yum, B. Koo, J. Lee, Genes Encoding the N -Acyl Homoserine Lactone-Degrading Enzyme Are Widespread in Many Subspecies of Bacillus thuringiensis. Appl Environ Microbiol. 68 (2002) 3919-3924.
13. A. Mohanty, C.H. Tan, B. Cao, Impacts of nanomaterials on bacterial quorum sensing: differential effects on different signals. Environ Sci Nano. 3 (2016) 351-356.
14. V.C. Kalia, Quorum sensing inhibitors : An overview. Biotechnol Adv. 31 (2016) 224-245.
15. W.R.J.D. Galloway, J.T. Hodgkinson, S.D. Bowden, M. Welch, D.R. Spring, Quorum Sensing in Gram-Negative Bacteria : Small-Molecule Modulation of AHL and AI-2 Quorum Sensing Pathways. Chem Rev. 111 (2011) 28-67.
16. D. Natrajan, S. Srinivasan, K. Sundar, A. Ravindran, Formulation of essential oil-loaded chitosan–alginate nanocapsules. J Food Drug Anal. 23 (2015) 560-568.
17. I.M Helander, E-L. Nurmiaho-Lassila, R. Ahvenainen, J. Rhoades, S. Roller, Chitosan disrupts the barrier properties of the outer membrane of Gram-negative bacteria. Int J Food Microbiol. 71 (2001) 235-244.
18. Y.J. Jeon, P.J. Park, S.K. Kim, Antimicrobial effect of chitooligosaccharides produced by bioreactor. Carbohydr Polym. 44 (2001) 71-76.
19. F. Devlieghere, A. Vermeulen, J. Debevere, Chitosan: antimicrobial activity , interactions with food components and applicability as a coating on fruit and vegetables. Food Microbiol. 21 (2004) 703-714.
20. H. Liu, Y. Du, X. Wang, L. Sun. 2004. Chitosan kills bacteria through cell membrane

damage. Int J Food Microbiol. 95 (2004) 147-155.

21. E.M. Costa, S. Silva, C. Pina, F.K. Tavaria, M. Pintado, Antimicrobial Effect of Chitosan against Periodontal Pathogens Biofilms. Symbiosis. 2 (2014)1-6.
22. D.R. Perinelli, L. Fagioli, R. Campana, J.K.W. Lam, W. Baffone, G.F. Palmieri, L. Casettari, G. Bonacucina, Chitosan-based nanosystems and their exploited antimicrobial activity. Eur J Pharm Sci. 117 (2018) 8-20.
23. M. Gouda, U. Elayaan, M.M. Youssef. Synthesis and Biological Activity of Drug Delivery System Based on Chitosan Nanocapsules. Adv Nanoparticles. 3 (2014) 148-158.
24. X. Qin, J. Emich, F.M. Goycoolea. Non-toxic chitosan with quorum sensing inhibition activity in a AHL-based E. coli biosensor. Submitted.
25. C. Vila-Sanjurjo, C. Remuñán-López, L. David, C. Rochas, F.M. Goycoolea, Interference with a bacterial quorum sensing-based response by sub-lethal levels of chitosan nanoparticles. Submitted.
26. X. Qin, C. Engwer, S. Desai, C. Vila-Sanjurjo, F.M. Goycoolea, An investigation of the interactions between an E. coli bacterial quorum sensing biosensor and chitosan-based nanocapsules. Colloid Surface B. 149 (2017) 358-368.
27. A. Adabiardakani, M. Hakimi, H. Kargar, 2012. Cinnamaldehyde Schiff Base Derivatives : A Short Review. World Appl Program. 2 (2012) 472-476.
28. T.B. Adams, S.M. Cohen, J. Doull, V.J. Feron, J.I. Goodman, L.J. Marnett, I.C. Munro, P.S. Portoghese, R.L. Smith, W.J. Waddell, B.M. Wagner, The FEMA GRAS assessment of cinnamyl derivatives used as flavor ingredients. Food Chem Toxicol. 42 (2004) 157-185.
29. S. Zinn, T. Betz, M. Schnell. 2015. Structure determination of trans-cinnamaldehyde by broadband microwave spectroscopy. Phys Chem Chem Phys. 17 (2015) 16080-16085.

30. C. Niu, S. Afre, E.S. Gilbert, Subinhibitory concentrations of cinnamaldehyde interfere with quorum sensing. Lett Appl Microbiol. 43 (2006) 489-494.
31. G. Brackman, T. Defoirdt, C. Miyamoto, P. Bossier, S.V. Calenbergh, H. Nelis, T. Coenye, Cinnamaldehyde and cinnamaldehydederivatives reduce virulence in Vibrio spp. by decreasing the DNA-binding activity of the quorum sensing response regulator LuxR. BMC Microbiol. (2008) doi:10.1186/1471-2180-8-149.
32. G. Brackman, S. Celen, U. Hillaert, S.V. Calenbergh, P. Cos, L. Maes, H. Nelis, T. Coenye, Structure-Activity Relationship of Cinnamaldehyde Analogs as Inhibitors of AI-2 Based Quorum Sensing and Their Effect on Virulence of Vibrio spp. PLoS One. 6(2011):e16084. doi:10.1371/journal.pone.0016084.
33. C. Chang, T. Krishnan, H. Wang, Y. Chen, W. Yin, Y. Chong, L. Tan, T. Chong, K. Chan, 2014. Non-antibiotic quorum sensing inhibitors acting against N-acyl homoserine lactone synthase as druggable target. Sci Rep. 4 (2014) 7245. doi:10.1038/srep07245.
34. C. Vila-Sanjurjo, C. Engwer, X. Qin, C. Remuñán-López, A. Vila-Sanjurjo, F.M. Goycoolea, Percolation theory can explain primordial forms of cell-to-cell communication. bioRXiv. doi: http://dx.doi.org/10.1101/074369
35. K. Ponnusamy, D. Paul, J.H. Kweon, Inhibition of Quorum Sensing Mechanism and Aeromonas hydrophila Biofilm Formation by Vanillin. Environ Eng Sci. 26 (2009) 1359-1363.
36. S. Norizan, W. Yin, K. Chan, Caffeine as a Potential Quorum Sensing Inhibitor. Sensors. 13 (2013) 5117-5129.
37. L. Zhang, D. Pornpattananangkul, C.J Hu, C. Huang, Development of Nanoparticles for Antimicrobial Drug Delivery. Curr Med Chem. 17 (2010) 585-594.

38. L.M. Lucht, N.A. Peppas, Transport of Penetrants in the Macromolecular Structure of Coals .V. Anomalous Transport in Pretreated Coal Particles. J Appl Polym Sci. 33 (1987) 1557-1566.

39. A. Kumari, R. Singla, A. Guliani, S.K. Yadav, Nanopartices for drug delivery. EXCLI J. 13 (2014) 265-286.

40. M. Kaiser, S. Pereira, L. Pohl, S. Ketelhut, B. Kemper, C. Gorzelanny, H.J. Galla, B.M. Moerschbacher, F.M. Goycoolea, Chitosan encapsulation modulates the effect of capsaicin on the tight junctions of MDCK cells. Sci Rep. 5 (2015) 10048. doi:10.1038/srep10048.

41. F.M. Goycoolea, A. Valle-gallego, R. Stefani, B. Menchicchi, L. David, C. Rochas, M.J. Santander-ortega M.J. Alonso, Chitosan-based nanocapsules : physical characterization , stability in biological media and capsaicin encapsulation. Colloid Surface B. 2 (2010) 1423-1434.

42. A. Gupta, H.B. Eral, T.A. Hatton, P.S. Doyle, Nanoemulsions: formation, properties and applications. Soft Matter. 12 (2016) 2826-2841.

43. R.S. Schuh, F. Bruxel, H.F. Teixeira, 2014. Physicochemical properties of lecithin-based nanoemulsions obtained by spontaneous emulsification or high-pressure homogenization. Quim Nov. 37 (2014)1193-1198.

44. M.J. Santander-ortega, J.M. Peula-garcía, F.M. Goycoolea, J.L. Ortega-vinuesa, Chitosan nanocapsules : Effect of chitosan molecular weight and acetylation degree on electrokinetic behaviour and colloidal stability. Colloid Surface B. 82 (2011) 571-580.

45. Š. Dalibor, I. Brabcová, A. Marou, P. Chocholou, P. Solich, Green chromatography separation of analytes of greatly differing properties using a polyethylene glycol stationary phase and a low-toxic water-based mobile phase. Anal Bioanal Chem. 405 (2013)6105-6115.

46. M.A. Franden, H.M. Pilath, A. Mohagheghi, P.T. Pienkos, M. Zhang, Inhibition of growth of Zymomonas mobilis by model compounds found in lignocellulosic hydrolysates. Biotechnol Biofuels. 6 (2013) 99.
47. N.T.T. Thanh, K. Bensadi, E. Dumas, A. Gharsallaoui, S. Gouin, M.H. Ly-Chatain, P. Degraeve, M.L. Thanh, N. Oulahal, Comparison of the antibacterial activity of Vietnamese Cinnamon essential oil and its chemotype (trans-cinnamaldehyde) in tryptone soya broth (TSB) and in an oil in water emulsion containing TSB : consequences for its use in food preservation. FOOD Sci Eng Technol. 60 (2013) 482-487.
48. T. Nii, F. Ishii, Encapsulation efficiency of water-soluble and insoluble drugs in liposomes prepared by the microencapsulation vesicle method. Int J Pharm. 298 (2005)198-205.
49. A. Mahapatro, D.K. Singh, Biodegradable nanoparticles are excellent vehicle for site directed in-vivo delivery of drugs and vaccines. J Nanobiotechnology. 9 (2011) 55.
50. Z. Yang, Z. Zeng, Z. Xiao, H. Ji, Preparation and controllable release of chitosan / vanillin microcapsules and their application to cotton fabric. Flavour Fragr J. 29 (2014) 114-120.
51. G. Wang, P. Li, Z. Peng, M. Huang, L. Kong, Formulation of Vanillin Cross-Linked Chitosan Nanoparticles and its Characterization. Adv Mater Res. 335-336 (2011) 474-477.
52. V.N. Babu, S. Kannan, Enhanced delivery of baicalein using cinnamaldehyde cross-linked chitosan nanoparticle inducing apoptosis. Int J Biol Macromol. 51 (2012) 1103-1108.
53. P. Suptijah, J. Djajadisastra, C. Kirana, H. Saputro, T. Hidayat, The Characterization and Effectiveness Penetrasion of Caffeine Trapped and Coated Chitosan Nanoparticles as Anti-Cellulite. J Nanosci Nanoeng. 1 (2015) 198-205.
54. Z. Zhang, S. Feng, The drug encapsulation efficiency, in vitro drug release , cellular uptake and cytotoxicity of paclitaxel-loaded poly (lactide)–tocopheryl polyethylene glycol

succinate nanoparticles. Biomaterials. 27 (2006) 4025-4033.

55. L. Peltonen, J. Aitta, S. Hyvönen, M. Karjalainen, J. Hirvonen, Improved Entrapment Efficiency of Hydrophilic Drug Substance During Nanoprecipitation of Poly (l) lactide Nanoparticles. AAPS PharmSciTech. 5 (2004)1-6.
56. T.S.J. Kashi, S. Eskandarion, M. Esfandyari-Manesh, S.M.A. Marashi, N. Samadi, S.M. Fatemi, F. Atyabi, S. Eshraghi, R. Dinarvand, Improved drug loading and antibacterial activity of minocycline-loaded PLGA nanoparticles prepared by solid/oil/water ion pairing method. Int J Nanomedicine. 7 (2012) 221-234.
57. E. Cauchetier, M. Deniau, H. Fessi, A. Astier, M. Paul, Atovaquone-loaded nanocapsules : influence of the nature of the polymer on their in vitro characteristics. Int J Pharm. 250 (2003) 273-281.
58. L.F. Dalmolin, N.M. Khalil, R.M. Mainardes, Delivery of vanillin by poly (lactic-acid) nanoparticles : Development , characterization and in vitro evaluation of antioxidant activity. Mater Sci Eng C. 62 (2016) 1-8.
59. S. Knauer, M. Epple, Calcium phosphate increases the encapsulation efficiency of hydrophilic drugs (proteins, nucleic acids) into poly(D,L-lactide-co-glycolide acid) nanoparticles for intracellular delivery. J Mater Chem B. 2 (2014) 7250-7259.
60. A. Loquercio, E. Castell-perez, C. Gomes, R.G. Moreira, Preparation of Chitosan-Alginate Nanoparticles for Trans- cinnamaldehyde Entrapment. J Food Sci. 80 (2015) 2305-2315.
61. S. Budiasih, K. Jiyauddin, N. Logavinod, M. Kallemullah, A. Jawad, A.D. Samer, A. Fadli Y. Eddy, Optimization of Polymer Concentration for Designing of Oral Matrix Controlled Release Dosage Form. UK J Pharm Biosci. 2 (2014) 54-61.
62. P. Calvo, J.L. Vila-Jato, J. Alonso, Evaluation of cationic polymer-coated nanocapsules as

ocular drug carriers. Int J Pharm. 153 (1997) 41-50.

63. P. Sahariah, V.S. Gaware, R. Lieder, S. Jonsdottir, M.A. Hjalmarsdottir, O.E. Sigurjonsson, M. Masson, The Effect of Substituent, Degree of Acetylation and Positioning of the Cationic Charge on the Antibacterial Activity of Quaternary Chitosan Derivatives. Mar. Drugs. 12 (2014) 4635-4658.
64. K.A.M. O'Callaghan, J.P. Kerry, Preparation of low- and medium-molecular weight chitosan nanoparticles and their antimicrobial evaluation against a panel of microorganisms, including cheese-derived cultures. Food Control. 69 (2016) 256-261.